International Journal of Speleology	41(2)	283-296	Tampa, FL (USA)	July 2012

Available online at scholarcommons.usf.edu/ijs/ & www.ijs.speleo.it

International Journal of Speleology

Official Journal of Union Internationale de Spéléologie

Spatially dense drip hydrological monitoring and infiltration behaviour at the Wellington Caves, South East Australia

Catherine N. Jex[1,2,3*], Gregoire Mariethoz[1,2,3], Andy Baker[2,3], Peter Graham[2,3], Martin S. Andersen[2,3], Ian Acworth[2,3], Nerilee Edwards[4], and Cecilia Azcurra[1,2,3]

Abstract:

Jex C.N., Mariethoz G., Baker A., Graham P., Andersen M.S., Acworth I., Edwards N. and Azcurra C. 2012. Spatially dense drip hydrological monitoring and infiltration behaviour at the Wellington Caves, South East Australia. International Journal of Speleology, 41(2), 283-296. Tampa, FL (USA). ISSN 0392-6672. http://dx.doi.org/10.5038/1827-806X.41.2.14

Despite the fact that karst regions are recognised as significant groundwater resources, the nature of groundwater flow paths in the unsaturated zone of such fractured rock is at present poorly understood. Many traditional methods for constraining groundwater flow regimes in karst aquifers are focussed on the faster drainage components and are unable to inform on the smaller fracture or matrix-flow components of the system. Caves however, offer a natural inception point to observe both the long term storage and the preferential movement of water through the unsaturated zone of such fractured carbonate rock by monitoring of drip rates of stalactites, soda straws and seepage from fractures/micro fissures that emerge in the cave ceiling. Here we present the largest spatial survey of automated cave drip rate monitoring published to date with the aim of better understanding both karst drip water hydrogeology and the relationship between drip hydrology and surface climate. By the application of cross correlation functions and multi-dimensional scaling, clustered by k-means technique, we demonstrate the nature of the relationships between drip behaviour and initial surface infiltration and similarity amongst the drip rate time series themselves that may be interpreted in terms of flow regimes and cave chamber morphology and lithology.

Keywords: fractured rock; carbonate aquifer; drip rate; karst; karstic aquifer

Received 23 February 2012; Revised 21 April 2012; Accepted 15 May 2012

INTRODUCTION

Karst regions represent significant geographical areas of potentially high rates of infiltration through fractured and karstified carbonate rocks and are recognised as a significant global groundwater resource (Worthington and Gunn, 2009), and yet the nature of groundwater flow paths in the unsaturated zone of such fractured rock is at present poorly understood. Traditional studies of groundwater dynamics in karst aquifers have typically been conducted in streams and underground rivers where the points of recharge and resurgence are known (or under investigation). Tracer experiments have been used to calculate transit times for these high flow components of the karst aquifer (Worthington & Ford, 2009; Shapiro, 2011) and to infer the nature and the extent of karstification in carbonate settings (Maurice et al., 2010). The heterogeneity of karstic aquifers is well-recognised (Perrin et al., 2003), but the focus is still largely placed on monitoring of fast drainage flow systems, conduits and channels, which may describe the behaviour of an important, but nonetheless, limited portion of the total karst aquifer water volume. Meanwhile, less attention is focussed on understanding water movement through fractures/fissures and finer matrix/micro fracture networks which may comprise a significant volume of water (Baker & Fairchild, 2012). As these studies are not able to observe flow and storage through rock matrix or these smaller fracture/fissure networks, they lack vital information, relevant to understanding flow through fractured rocks in its entirety (Worthington & Ford, 2009). This is especially important in scenarios where the karst aquifer is found to have a high level of tracer attenuation, inferring the loss of tracer from large channels into smaller fracture/fissure network, and unknown points of resurgence or transit times (Maurice et al., 2010). This has significant implications for example in tracking pollution in karst regions. Further, these tracer studies are typically conducted during discrete monitoring periods that give information at a particular point in time and

[1]Water Research Centre, School of Civil and Environmental Engineering, University of New South Wales, Sydney, New South Wales, 2052, Australia (c.jex@unsw.edu.au).

[2]Connected Waters Initiative Research Centre, University of New South Wales, 110 King Street, Manly Vale, New South Wales, 2093, Australia.

[3]Affiliated to the National Centre for Groundwater Research and Training (NCGRT), Australia.

[4]Douglas Partners Pty Ltd, 96 Hermitage Road West Ryde, New South Wales, 2114, Australia.

space, and unless repeated, cannot tell us anything on seasonal or inter-annual to decadal timescales relevant for understanding longer term dynamics of groundwater recharge or infiltrating water transit times.

A recently published exception to this was a tracer study conducted in a cave at Mount Carmel, Israel, that measured drip water rates and chemistry of stalactites, soda straws and seepage from fractures/ micro fissures that emerge in the cave ceiling. (Arbel et al., 2010). In this study, uranyl (UO_2^{2+}) tracers were injected into soil pockets overlying the cave prior to a predicted rainfall event and monitored nine drip water sites and their tracer concentrations under these "natural" rainfall conditions (i.e. no artificial flushing which would otherwise induce artificially high flows). They constrained the flow-through times and mechanisms in the epikarst and vadose zone. In this way they were able to observe the infiltration response to surface climate after passing through the micro- and macro-fracture network for this Mediterranean karst system and made inferences on both the long term storage and the preferential movement of water through the unsaturated zone of such fractured carbonate rock. However, the study preferentially selected sites that were actively dripping, and so is limited in its ability to upscale the observations to describe water flow through the karst aquifer on a larger spatial scale. In the same region, another study went some way to address this, by using PVC sheeting in two areas of the cave to integrate water collection over multiple drip sites (in the order of 100 drips and up to 52 m^2) (Sheffer et al., 2011). Again three flow regimes were identified (see Table 1) and a rainfall threshold of approx. 100 mm at the start of the rainy season was estimated as necessary to replenish soil and epikarst storage and to initiate dripping in the cave. However, integrated water sampling is not able to provide details on the full range of individual drip responses or investigate spatial relationships between drip sources.

There is now several decades of publications of drip rate monitoring in caves for the purpose of characterising flow through the unsaturated zone which have led to our understanding of drip behaviour and expected observations in cave drip waters. Table 1 provides details of some of these, though it is by no means exhaustive. From initial studies that pioneered the measurement and characterisation of cave drip waters (Pitty, 1966, 1968; Gunn, 1974; Smart & Friederich, 1987), the more recent studies of (Genty & Deflandre, 1998; Baker & Brunsdon, 2003) identified the non-linear behaviour of cave drips as observed in larger karst springs. They demonstrated intra- and inter-annual drip discharge variability to be driven by periods of soil moisture excess. Further, they showed smaller scale drip variability to follow changes in atmospheric pressure and hinted towards the potential for chaotic behaviour of drip regimes due to non-linearity in the initial input (i.e. the weather) and / or the karst system. Drip classification schemes were proposed, based on mean discharge (Q) and some measure of flow rate variability (e.g. a coefficient of variability, i.e. standard deviation of Q normalised

Table 1. A summary of published and unpublished sources of cave drip rate monitoring data for the purpose of characterising flow regimes in the unsaturated zone of karst aquifers. This table is not an exhaustive summary, but highlights some key studies from around the world.

Author	Cave Region	Monitoring Period (yrs)	Method		Sampling Interval	Total number of monitoring sites	Number of automatic monitoring sites
Genty and Deflandre, 1998	France	5	Auto	Tipping bucket	10 min	1 drip	-
Baker & Brundson, 2003	N England	4	Auto	Tipping bucket	15 min	6 drips	Not stated
Fairchild et al. 2006	S England	2	Manual	Stopwatch	-	15 drips	-
Baldini et al., 2006	SW Ireland	3	Manual	Calibrated bottle (rapid drips) and stopwatch (slow drips)	-	Not stated	-
Fernandez-Cortez et al., 2007	SE Spain	4	Auto	Unknown automated logging system	1 hr	1 drip	1 drip
MacDonald & Drysdale, 2007	SE Australia	4	Auto	Unknown automated logging system	Unknown	10 drips	Not stated
Fuller et al., 2008	NW Scotland	2	Manual	Stopwatch	-	14 drips	-
Hu et al., 2008	Central China	3	Manual and Auto	Stopwatch and unknown automated logging system	10 min (auto)	Unknown number of drips	-
Miorando et al., 2010	NE Italy	3 yrs (auto) 6 yrs (manual)	Manual and Auto	Stopwatch and Stalagmate™	1hr (auto)	11 drips	Not stated
Treble et al., unpublished	SE Australia and W Australia	5 (manual) <1 (auto and ongoing)	Manual and Auto	Stopwatch and Stalagmate™	15 min (auto)	3 drips	3 drips
Jex et al. unpublished	SE Australia	1 (ongoing)	Auto	Stalagmate™	15 min	> 30 drips	> 30 drips
Pronk et al., 2009	Jura Mountains, Switzerland	2 x 0.5	Auto	Unknown automated logging system	Unknown	1 drip	1 drip
Arbel et al., 2010	Northern Israel	3	Auto	Tipping bucket (8 ml capacity)	Variable (10 mins to a few hours)	9 drips (stalactites located on a single speleothem formation)	9 drips
Sheffer et al. 2011	Northern Israel	3	Auto	Pressure transducer in a water collection barrel	5 min	3 integrated areas of multiple (10^2) drips, collected on PVC sheeting.	
Riechelmann et al., 2011	NW Germany		Manual (7 drips) and Auto (2 drips)	Stopwatch and Stalagmate™	-	7 drips in 2 cave chambers	2 drips

by the mean Q) in order to classify the nature of the drip response to surface climate (Smart & Friederich, 1987; Baker & Brunsdon, 2003). Subsequently, inferences on the complexity of flow routes, and hypotheses on drip chemistry according to flow routes were made, and are still referred to today. These original classifications were based largely on manually timed drip rate data, made on a monthly basis. The authors are not aware of any study to replicate these classifications, using a spatial set of drip rate monitoring that using continuous, automatically logged, drip rate data. It may be that such data no longer falls into these original classifications.

Water percolating as drip water into caves is likely to have routed via potential groundwater stores, of various sizes, such as solutionally widened fractures and proto-caves. Tectonic history (determining the density of fracture/joint networks), karstification (related to the extent of dissolution), and the age of the limestone (indicative of the extent of primary porosity as well as palaeokarst) will all determine the nature of this unsaturated zone hydrology. For instance, at one extreme, the dominance of micro-fractures or storage via primary porosity enables the slow transmission of water. From initial meteoric infiltration to emergence in the cave as drips, water residence times may be in the order of years or decades (Kaufman et al., 2003; Kluge et al., 2010). As a consequence, drip rates may be low with little intra- and inter-annual variability and the chemistry (isotopes, major ions) may demonstrate little intra-annual variability due to the long residence times of these waters allowing them to be chemically and isotopically well mixed. In contrast, drips which are predominantly fed by solutionally enhanced fractures, with limited stored water, may respond rapidly to infiltration, demonstrating variability in drip rates which may be seasonal or driven by individual infiltration events. Finally, one may hypothesise that, in older limestone which has undergone multiphase karst development that pockets of storage capacity can also be provided by sediment-filled palaeokarst. Water percolating from these stores is likely to demonstrate drip behaviour similar to that derived from primary limestone porosity, but chemistry that could be distinctive of the palaeokarst fill. Depending on the size of any particular water store, there may be a common response that is applicable to a group of drips observed within a cave system. In all of these cases seasonal or event based thresholds of soil moisture may be critical in determining onset of drip response.

The extent to which these different flow routes are significant at specific cave sites has yet to be directly observed, as cave based monitoring programs that utilise automated continuous data logging are often restricted to monitoring a single drip (Genty & Deflandre, 1998; Fernández-Cortés et al., 2007) or a maximum of ~10 drips (Fuller et al., 2008; Arbel et al., 2010; Miorandi et al., 2010) (Table 1). Crucially, the study of cave drip waters over a significant area of a single system should be useful in understanding when and how infiltration of cave drip waters in a karst area occurs; producing a dataset of continuous observations at a sub-hourly temporal resolution that can be used to develop site specific conceptual models and calibrate numerical models of these systems. Automated drip rate logging systems are also a prerequisite in order to make quantitative comparisons between drip rate and surface climate parameters (rainfall and pressure) and to within cave micro-climate parameters (pressure, temperature and CO_2 as an indicator of cave air ventilation) which may drive additional geochemical reactions or rate changes in drip waters. With the availability of new drip rate logging devices it is now possible to deploy many of these devices for larger scaled spatial studies of many individual drips.

With the aim of improving our understanding both of karst drip water hydrogeology and the relationship between drip hydrology and surface climate, we present here the results of the first year of a long-term monitoring study of drips in a single chamber of the Cathedral Cave, part of the Wellington Caves system in the state of New South Wales, Australia. Here we present:

1) The largest data set of continuous drip rate monitoring data, now freely available with the publication of this study.

2) New data on the hydrological behaviour of cave drips when measured at high sampling density.

3) Novel application of existing statistical techniques to address the potential of such techniques to classify, quantify and visualise the observed relationships between infiltration through the fractured limestone rocks and initial surface climate inputs.

SITE DESCRIPTION

Studied Cave

Cathedral Cave, one of many caves that form part of the larger Wellington Caves Reserve (32°37'S; 148°56'E) is located west of the Blue Mountains, part of the Great Dividing Range mountain belt that runs approximately North-South along the Eastern sea-board of Australia. The caves are approximately 7 km south of the town of Wellington, New South Wales (Fig. 1) and Cathedral Cave is a show cave, open to tourists daily. The caves are developed in dense, deformed Devonian limestone, at the boundary between two distinct facies: a massive, marmorised lime-mudstone comprising pelletal, oolitic and algal calcarenite (Frank, 1971; Frank, 1975) and a more extensive thinly bedded limestone, comprising graded beds with faecal pellets (Osborne, 2007). Orogenetic development during the mid-Devonian and early Carboniferous resulted in widespread folding, including the Lachlan fold belt in which the caves are situated (Osborne, 2007). Caves development is promoted along faults and joints, with evidence of the importance of both meteoric water and groundwater in cave formation (Osborne, 2007). The widespread presence of palaeokarst in the caves also suggests several phases of cave development, and as such the Wellington Caves are likely to be fairly typical of Devonian and Silurian limestones in Eastern Australia. A number of possible flow routes are likely, including drips fed by waters transmitted

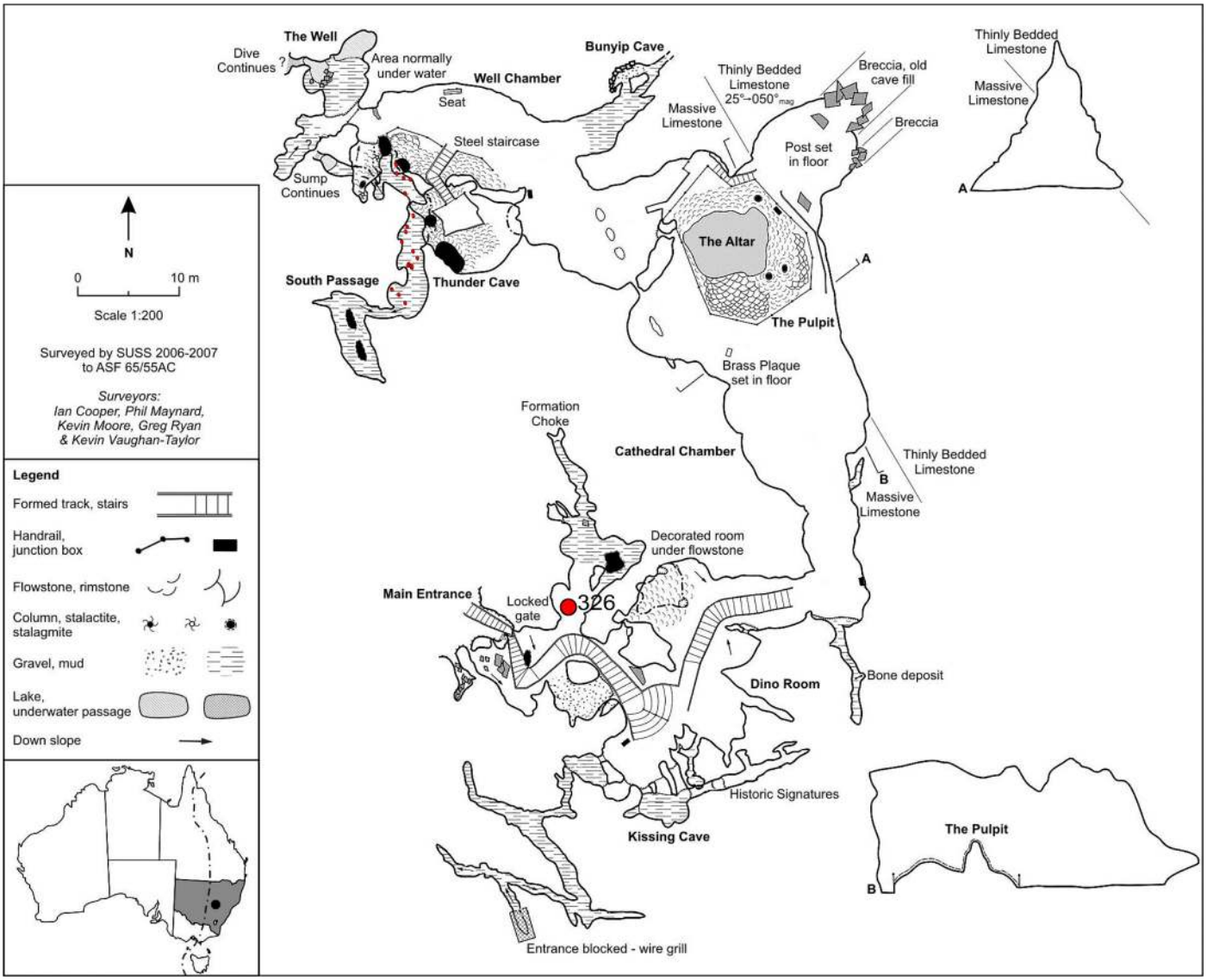

Fig. 1. Location map of the Wellington Caves and survey of Cathedral Cave. All drip loggers were located in the South Passage, part of the deeper section of the cave at approximately 30 m below the surface. Directly above this portion of the cave is a slight depression with deeper soil development and patchy, shrub vegetation, which is likely to act a focus point for infiltration above South Passage.

through solutionally widened fractures and proto-caves, fractures and micro fractures, palaeokarst fill or flow through the limestone matrix. The caves intercept the modern day water table, and whilst dry for most of the year, may be prone to flooding during extreme rainfall.

The locations of the drip loggers are shown in Fig. 1, and in detail with site descriptions in Fig. 2a and b. All selected monitoring sites are drip waters, which display a range of stalactite morphologies (stalactites, soda straws and seepage points with no soda-straw development). Likewise many sites have corresponding stalagmites of varying dimensions, though largely this comprises fresh growth of just a few mm. Many of the stalactites had been recently broken, presumably during show cave development and use in the early 20th century. More drip loggers are shown in the photos contained within these figures than are presented in this paper; multiple logger failures limited the number of continuous datasets during 2010, and just eighteen continuous series are presented here. In the data presented here, all except one logger are located in the South Passage of Cathedral Cave. In South Passage, the chamber roof comprises the base of a massive paleokarst infill, and consists of consolidated, interbedded sediment and flowstone layers. Overall Cathedral Cave has little speleothem decoration with a few notable areas of exception: active deposition in the South Passage chamber and on the large column and flowstone referred to as “The Altar” in Fig. 1; and an inactive speleothem filled chamber under flowstone nearer to the cave entrance (Fig. 1). At the ground surface above the South Passage there is a very shallow depression, which is likely to act as a small catchment in which infiltration is focussed. This could explain why this section of the cave is hydrologically more active compared to the rest of the cave system.

Above the cave, the surface comprises of open native Australian woodland including trees of black cypress, white cypress, kurrajong, silky oak and a few remnant white and yellow box gums. The ground cover is mainly native grass. The soil is described as aeolian red clay which is typical of SE Australia, with some outcropping limestone. The soil layer is mostly thin, with the deepest profiles located in limestone grikes and dolines (typically < 1m soil depth).

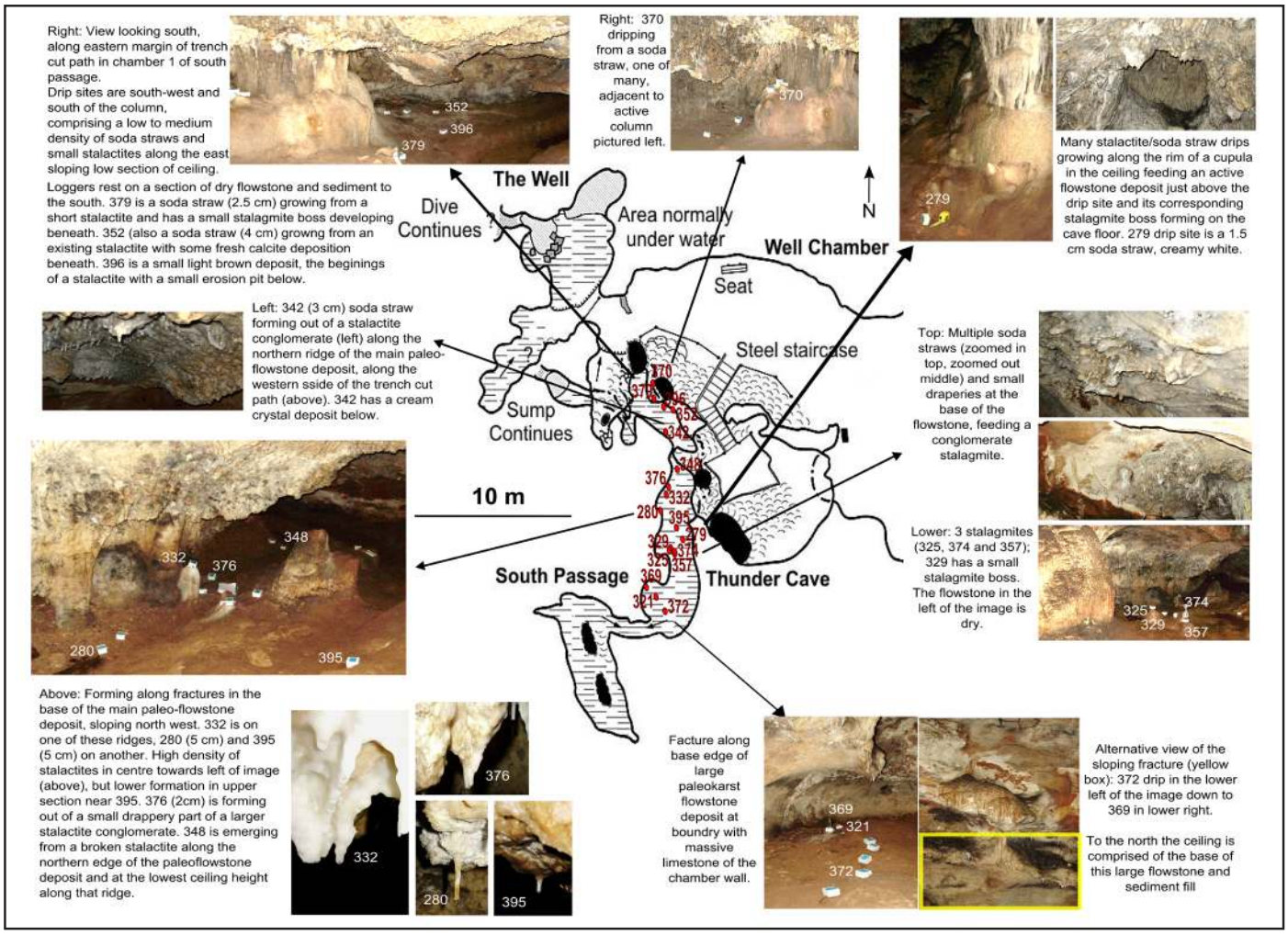

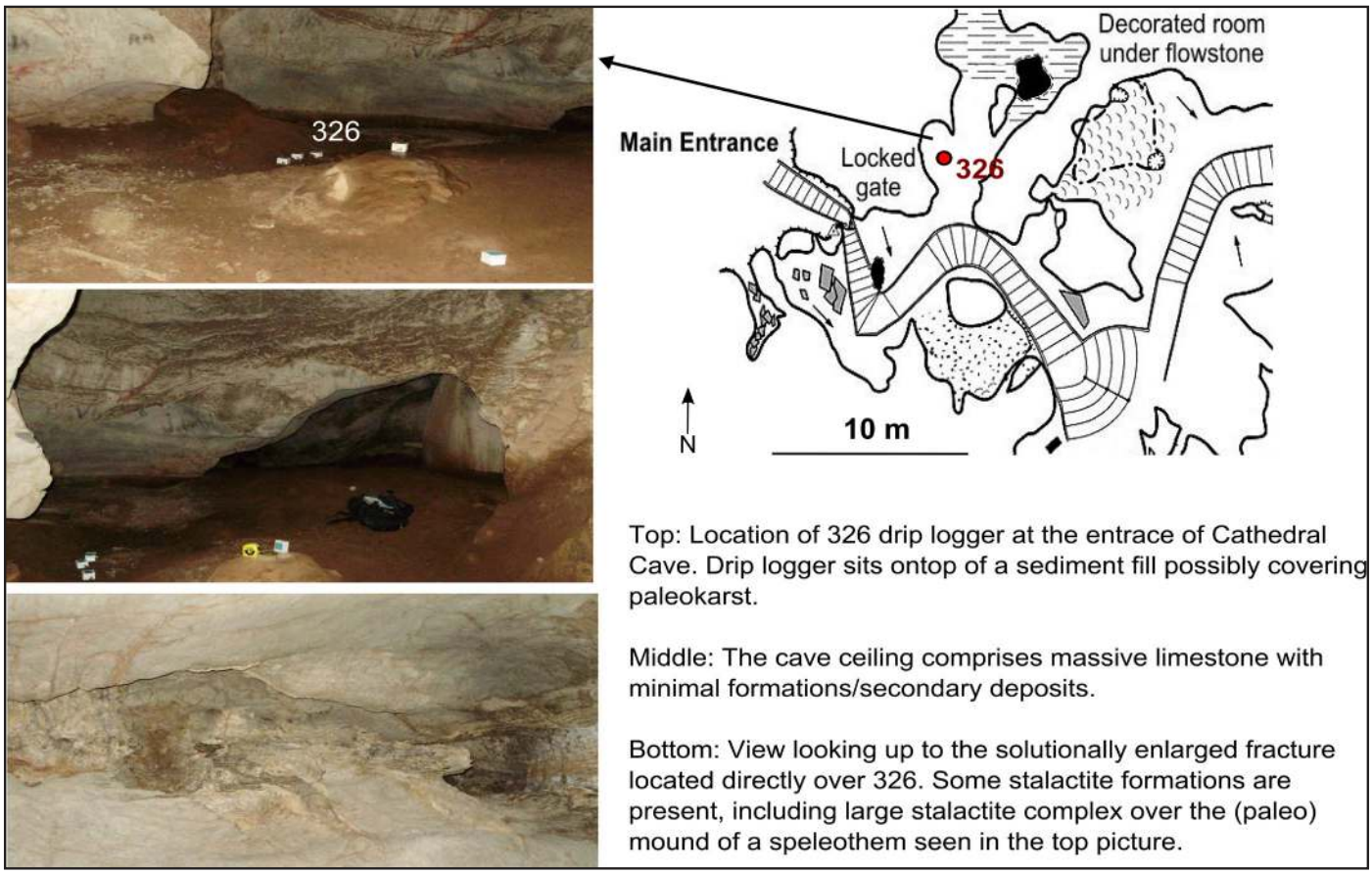

Fig. 2. Drip logger locations in (a) South Passage and (b) at the cave entrance, with site descriptions.

Climate and Meteorology

The nearest meteorological station (Station Number: 65034) is located at Wellington Agrow plow (lat: 32.56°S / Long: 148.95°E / 350 m asl), 6.5 km from the caves. Wellington falls within the temperate climate zone of Australia, receiving rainfall all year round (mean annual total approx. 620 mm (for the years AD 1881 to 2010), but a strong seasonality in temperature regime results in a soil moisture deficit for most of the year as shown in Fig. 3a. Based on the equations of Thornthwaite & Mather (1957) for evapotranspiration and based on the assumptions in Genty & Deflandre (1998) a soil moisture deficit (precipitation (mm) minus estimated evapotranspiration (mm)) is suggested to have lasted until May 2010, after which an unusually prolonged period of water excess is estimated for the site until the end of this dataset in late 2010. This is likely to exceed the seasonal threshold for infiltration and drip logger response at the study site. The year monitored, was one of the wettest years on record, following on from Australia's most recent 10 year drought (*"the big dry"*, Fig. 3b), ending with a period of major flooding throughout Eastern Australia as a whole in December 2010, which forced an interruption in monitoring at this site, as the water table rose and flooded the South Passage up to the elevation of the Altar (Fig. 1), in Cathedral Cave. The floods were themselves largely due to a prolonged wet winter and autumn, which maintained a higher than normal water table, soil moisture, dam and river levels throughout many of the affected catchments in late 2010. Over the last century, Wellington has recorded many of the large and extensive periods of droughts to have affected SE Australia as well as flooding events of similar and greater magnitude than those observed in December 2010 (Fig. 3b).

METHODS

Field Methods

A total of eighteen drip monitoring sites were established at the start of the hydrological year in May 2010 and June 2010. A further thirty-eight sites have since been established and are currently being monitored, but this data is not presented here. Stalagmate® drip loggers (www.driptych.com) were installed at almost every practical location throughout the South Passage chamber of Cathedral Cave (Fig. 1). The practicality of drip logger location was determined by drip height and the isolation of the drip. A height of 1 m between drip logger and stalactite tip is recommended to provide sufficient potential energy for reproducible results over a range of drip rates and volumes (Collister & Mattey, 2008), though we found that typically a height > 20 cm was sufficient. Drip isolation refers to the proximity of the drip being monitored to other drips (active and non-active) as such drips have potential for recording the response of multiple drips on a single logger, which may have been inseparable in the recorded data). Data loggers were set to record continuously at 15 minute intervals. The output data is therefore the number of drops that fell on the logger per 15 minutes. Full details of each logger location and setting are provided along with the drip data.

Data Treatment and Statistical Methods

Data was downloaded just prior to the large floods of early December 2010. Data recorded during periods of known fieldwork were removed from the drip rate time series, including 1 day either side of recorded field trip days as standard protocol.

The 15 minute data logging interval and the number of loggers used in this study results in a significant amount of data for the period considered. The following statistical and visualisation tools were employed: (1) cross-correlation functions for identifying temporal offsets in hydrological response; (2) a combination of multi-dimensional scaling (MDS) and k-means algorithm for clustering the loggers (Borg & Groenen, 1997; Scheidt & Caers, 2009).

Cross-correlation functions:

The correlation function refers to the correlation between two time series when these are shifted by different lags. It is possible, for example, that a high correlation can be found when the series are shifted by a significant amount, meaning that one of them has a response that is delayed compared to the other, but that both series have similar controlling mechanisms.

MDS and k-means algorithm:

For ease of visualisation and to undertake statistical analyses of the large dataset (close to 15'000 individual data points for 18 loggers during the monitoring period), we employed MDS. MDS starts by defining a distance between a set of objects. In this case each drip logger is

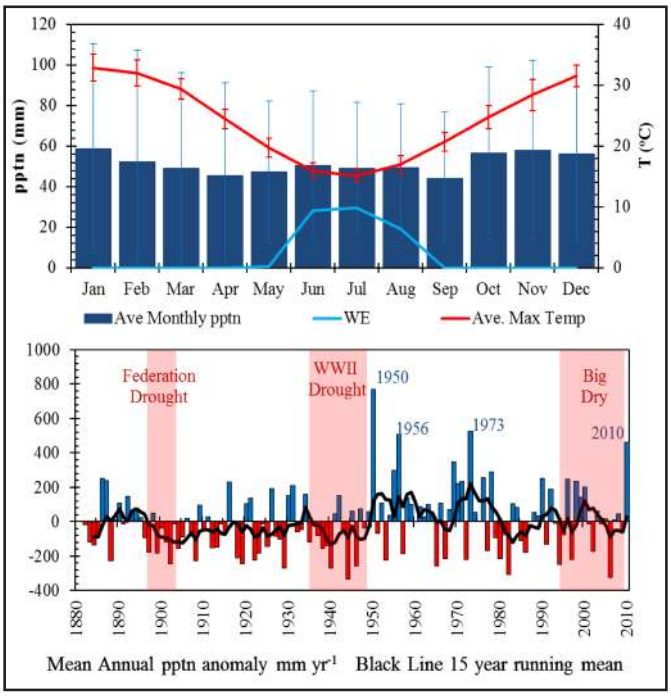

Fig. 3. Climatology of Wellington Caves region. Estimated water excess via the equation for estimated evapotranspiration of Thornthwaite & Mather (1957) according to the assumptions of Genty & Deflandre (1998), plotted alongside mean rainfall and temperature for the entire instrumental record. Historical precipitation data. Mean annual anomaly with respect to the entire period on record is plotted as bars, with a 15 year moving average in black.

an object and a specific distance between drip loggers is considered. To define appropriate similarity measures between loggers, we determined some factors that may help determine the degree of similarity between two drip logger time series:

1. The offset *O* (in hours) needed to align two time series such that they present maximum correlation. This value is determined with a 2-step algorithm consisting in a) computing the cross-correlation function between both time series and b) defining *O* as the lag time associated with the maximum correlation.

2. The complement of the correlation coefficient (*R*) between both series (such that large coefficient corresponds to a small distance and vice versa). More precisely, this complement of correlation is defined as 1 – *R*, where *R* is the correlation coefficient after the series has been shifted to obtain the maximum correlation coefficient (as in 1).

The factors 1 and 2 above mean that to be similar, two time series should be highly correlated, but in addition it is desirable that this correlation is obtained by applying a small offset. It should be noted that the MDS method requires a distance matrix to be applied, in which a single scalar number characterizes the similarity between any two loggers. Therefore, we need to formulate a single distance measure taking account for these criteria. The offset *O* should be considered as a discriminating measure only when the complement of correlation is high. If the correlation is low, any offset value, whether small or large, can be considered insignificant. Therefore we calculate the distance by considering the offset *O* and weighting it with the complement of correlation (equation 1).

$$d = O\,(1 - R) \qquad (1)$$

Where *d* is the defined distance, in this case the correlation-offset distance with which two similar time series (i.e. any of the drip rate time series) should be highly correlated and also present a small lag with each other.

With this specified distance measure, a distance matrix is computed containing the distance between each pair of loggers. MDS is used to translate a distance matrix into a configuration of points defined in an n-dimensional Euclidean space (Cox & Cox, 1994; Borg & Groenen, 1997). The points in this spatial representation are arranged in such a way that their respective Euclidean distances correspond as much as

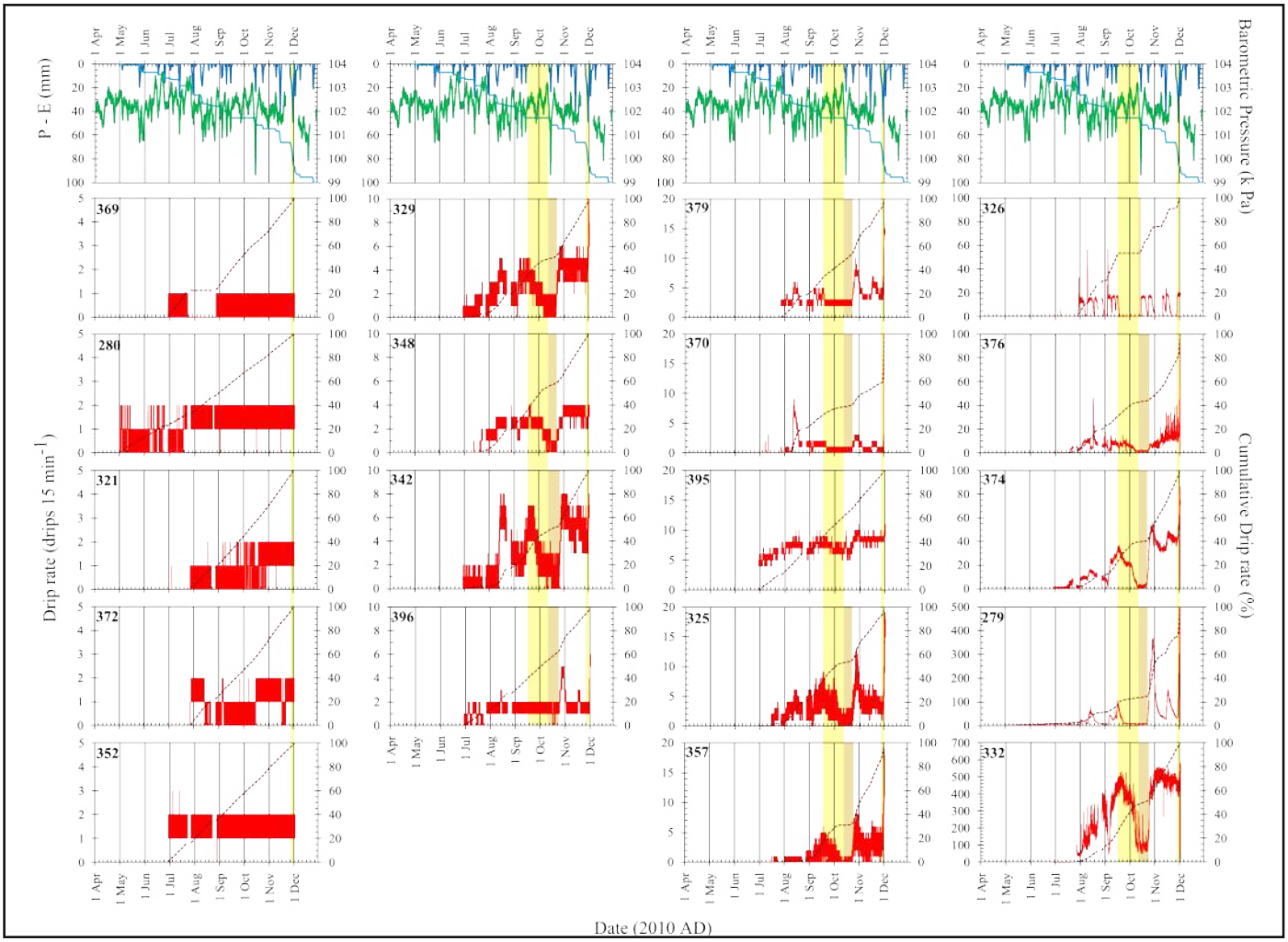

Fig. 4. Drip rate time series (solid red) and cumulative profiles of drip rate data (dotted red) plotted alongside the relevant climatic parameters of P-E (solid blue), cumulative P-E (light blue) and barometric pressure (green). The yellow highlights indicate two common features of the rainfall regime that year, including a dry spell in mid-September to October (brown shading indicates the delayed nature of the drip response to this period) and the late November-early December floods of 2010.

possible to the dissimilarities of the objects. The MDS algorithm can be posed as an optimization problem, which is solved here using a least-squares method, but in fact other optimizations could be employed. The result is a set of coordinates that defines the position of each drip in this high-dimensional distance space. Note that since the map obtained by MDS is based only on the dissimilarity distances in the matrix, the absolute location of the points is irrelevant. The map can be subject to translation, rotation, and reflection, without impacting the methodology. Only the distances in mapping space are of interest. Once the time series are located in this distance space, they are clustered with the k-means technique (Spath, 1985). The idea here is that it is possible to use a specific distance for clustering that incorporates criteria relevant for discriminating between drips.

RESULTS AND DISCUSSION

Drip Rate Time Series

The drip rate time series are plotted alongside daily rainfall totals (and cumulative rainfall expressed as a percentage of total rainfall between May to Dec that year i.e. since the start of that hydrological year) in Fig. 4. Also shown is the cumulative drip rate (expressed as a percentage of total drips since the start of monitoring). As the Thornthwaite method for calculating PET is not able to estimate values at sub-monthly resolution, a crude estimate of hydrologically effective precipitation, precipitation minus evaporation (referred to as P – E, measured in mm per day) was used. These values were interpolated to 15 minute interval time series for comparison with drip rate data in the cross correlation and MDS analyses.

Despite the high spatial density of loggers within what would appear to be a single area of palaeokarst fill, they do not demonstrate a single discharge response to hydrologically effective precipitation, instead displaying an apparently diverse range of drip rates, with variations in the range, mean and standard deviation (Fig. 4 and Table S1 in supplementary information). In Fig. 4 (last column), only two loggers exhibit a clear response to rainfall for the entire duration of the monitoring period. One is not located within South Passage and is close to the surface (logger 326). This drip responds very suddenly to recharge, in contrast to other sites of similar drip rates. Often they record an initial pulse of increased dripping within hours of initial infiltration, and then maintain a steady rate of dripping, typically for a few days, followed by a receding limb. Such a response is typical of water sourced from fracture flow, with limited storage capacity. The other is logger 279, within South Passage, which exhibits a series of classic hydrograph responses from August to the end of the logging period.

At the other extreme, some monitoring sites with very low drip rates (Fig. 4 and S2 in supplementary information, first column) exhibit a near constant drip rate with little or no relationship to hydrologically effective precipitation (as indicated by the almost linear nature of the cumulative drip profiles). All other drip loggers exhibit a trend to increasing drip rate during the course of monitoring.

Cross Correlation Functions with atmospheric variables

It is expected that due to the inertia of subsurface flow processes, the karst system will show a delayed response to any recharge event or change in atmospheric pressure. Therefore we used cross-correlation functions to determine the correlation between atmospheric variables and drip rate for different lag times. As described above, correlations to P–E in the majority of all drip rate time series are too low to be considered meaningful. However, the rapid response of some drips (370, 326, 279, 379, 376, 357 and 325) to the floods of December 2010 can be seen in Fig. 4. In these cases, these extreme drip rates are enough to produce artificially high correlation coefficients that are entirely due to this short period of fast dripping during this extreme event (Fig. 5a). These correlations no longer exist once the 5% most extreme drip rate data are removed in all but logger 326 (Fig. 5c). One possible explanation is that a dual flow regime exists in these drips, with pressurised saturated flow possible during extreme recharge events, and unsaturated percolation under normal to low recharge conditions with presumably a seasonal threshold.

Fig. 5b and 5d illustrate a negative correlation between some of the drip rate time series and barometric pressure as measured at the Baldry meteorological station (approx. 20 km away). This is the nearest station to record sub-daily barometric pressure and should be a reflection of any pressure changes at the surface above the cave. A negative correlation between drip rate and pressure with no (or a low) lag, would be indicative of two-phase-flow previously observed in French and British caves (Genty & Deflandre, 1998; Baker & Brunsdon, 2003; Fernández-Cortés et al., 2007; Verheyden et al., 2008). This is a direct process, whereby expansion or compression of air bubbles in the water is driven by local changes in atmospheric pressure, and either promotes or suppresses dripping (Genty & Deflandre, 1998). Loggers 395 (R = – 0.5, lagged by 10 hours) and 396 (R = – 0.34, lagged by 10 hours) are the only loggers here to clearly demonstrate this type of direct response to pressure. An indirect relationship may also be seen in loggers that have a lagged negative correlation to pressure, and increased dripping after rainfall. For example, logger 326, demonstrates a relatively strong correlation to pressure (R = –0.52) but highly lagged (up to 40 hours). Finally many loggers show very long lags or no correlation at all, and such behaviour is as yet unexplained.

The relationship between barometric pressure and drip rates is in some cases affected by the removal of extreme values (for example loggers 374 and 357 in Fig. 3e). Broadly speaking however, changes in pressure do not play a direct role in sudden discharge increases for the majority of loggers. Only two sites demonstrate a clear direct response of drip rate to changes in pressure. There is however, evidence for pressure to be associated with some fluctuation in drip rate in a few sites which may be indirectly related to rainfall. It should also be noted that despite some evidence of response to atmospheric pressure in a

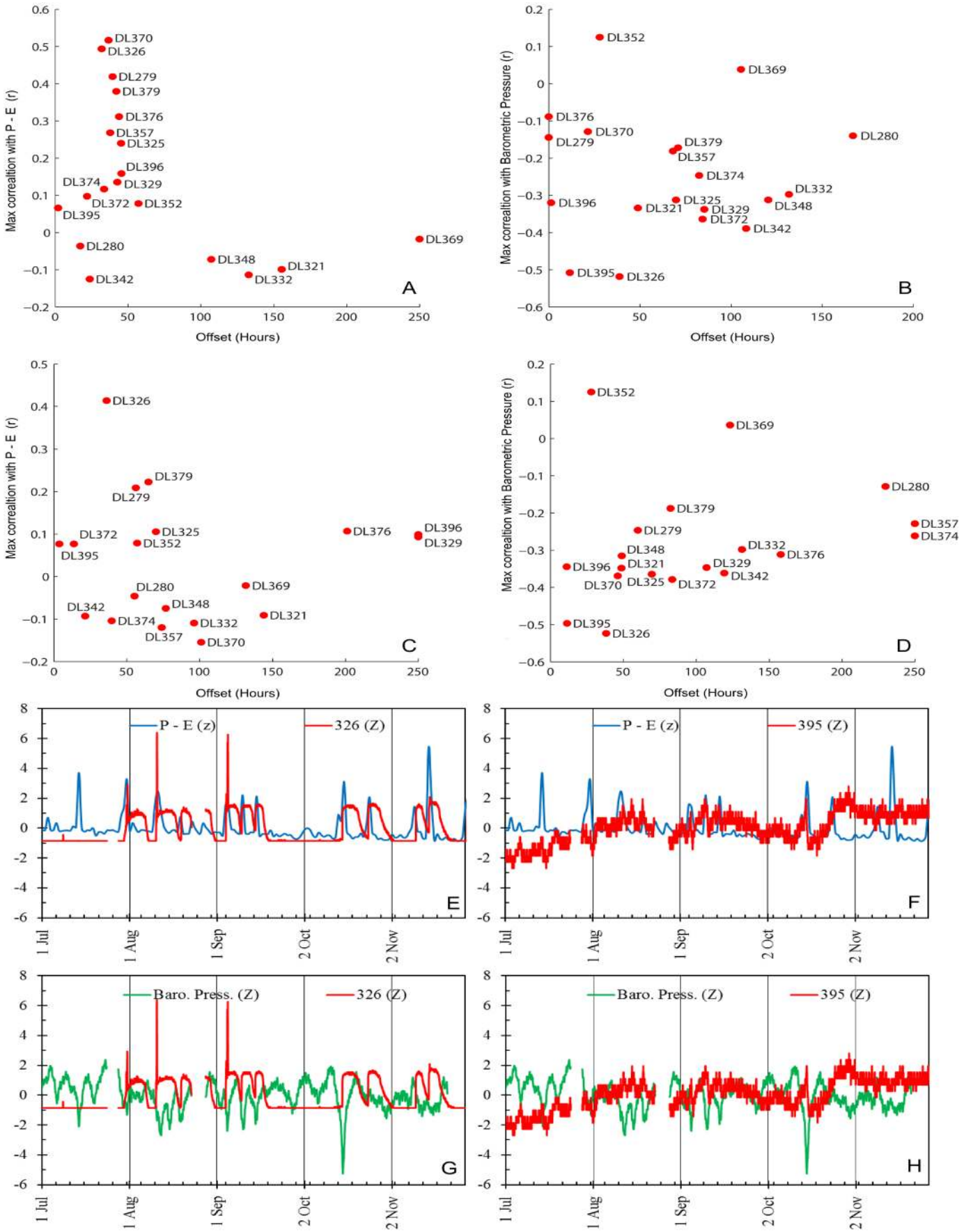

Fig. 5. Cross correlation relationships between (a) surface infiltration (P-E) and drip rate time series using all data; (b) barometric pressure and drip rate times series using all data; (c) surface infiltration (P-E) and drip rate times series after the removal of the top 5% of extreme values, and (d) barometric pressure and drip rate times series after the removal of the top 5% of extreme values. Standardised time series (using mean and standard deviation from 1st July to 1st December inclusive) are also presented in (e) to compare P-E and drip logger 326; (f) to compare P-E and drip logger 395; (g) to compare barometric pressure and drip logger 326, and (h) to compare barometric pressure and drip logger 395.

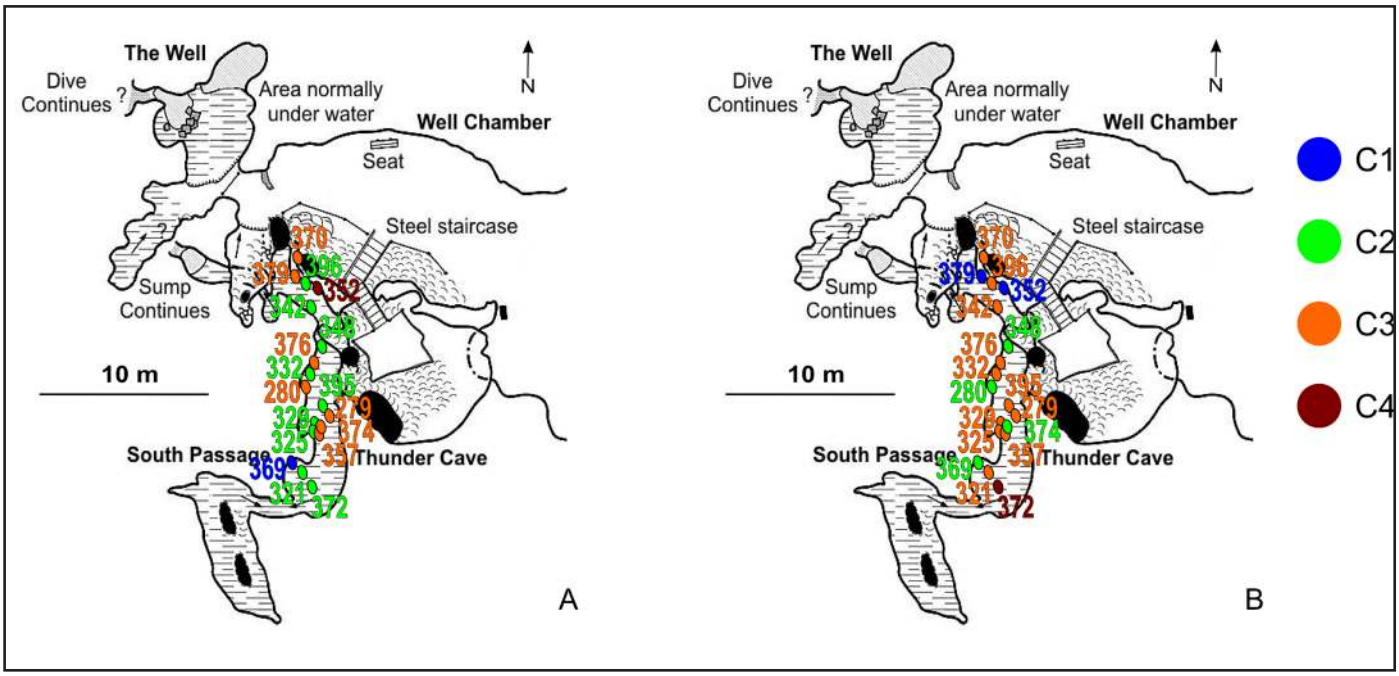

Fig. 6. Results of the MDS according to the correlation-offset distance and clustering plotted overlain upon the cave survey for the South Passage. All data (a) and filtered data (b), where the top 5% of extreme values have been removed. Details of the cluster parameters are provided in Table 2.

limited number of drips, spectral analysis of all the drip rate time series (not shown) did not demonstrate any periodicity associated with earth tides as previously noted for groundwater in confined aquifers (Acworth & Brain, 2008).

MDS: Similarity between the drip logger times series

Given the variability in the response of any individual drip logger, MDS analyses are employed to see if such an approach can identify any similarities amongst these time series, and cluster the data accordingly. As described earlier, the data are clustered according to similarity in the correlation-offset distance between the logger time series. In the k-means clustering algorithm, the number of clusters should be significantly smaller than the number of samples, we therefore imposed 4 clusters. Results are plotted spatially, overlaid on the South Passage survey in Fig. 6 and summarised in Table 2. Note that logger 326 is not plotted as, for simplicity; we focus on the loggers located within South Passage. Drip logger time series are deemed similar if they are well correlated and only have a small offset with each other, and so these loggers should cluster together. Others loggers may cluster if their correlation is very low but their relative offset is very high (or the opposite), or if they simply do not quite fit in with other clusters. These do not constitute physically meaningful clusters and so in order to differentiate between such scenarios and to make a physical interpretation based on this, we use the mean distance between samples within a cluster (the correlation-offset relationship as defined in equation 1) as an indicator of the quality of any cluster, i.e. the smaller the mean distance the more compact the cluster and the more believable it is. Also listed in Table 2, are the mean correlation coefficient within each cluster and the mean offset in the cluster. Viewed in this way, clusters are apparent spatially, and are dependent on whether or not all the data or the filtered data set (with removal of the top 5% of extreme values in the December floods) are used.

If all the data are used, then most of the loggers that record a response to the December floods cluster together in C3, which has the smallest mean distance parameter, a reasonable correlation and the shortest offset time of all the clusters. This cluster therefore reasonably represents this proportion of drip sites which had a fast response to surface infiltration during such an extreme event as described earlier, presumably via a well-connected fracture network, or at least fractures that may be disconnected but none the less, behave similarly. On removal of the top 5% extreme values, this cluster retains many of these dual regime drip sites, but gains loggers that were previously clustered separately if all data are used. It has the smallest distance measure of all clusters for these filtered data, with a strong correlation and now a larger offset of around 79 hours. This indicates that these fracture fed drips behave similarly to each other, even with the removal of the dominant December flood event, but that there is a much greater heterogeneity in flow routes of water under more “normal” unsaturated flow conditions. The majority of these drips are located at the base of the massive palaeoflowstone, whilst other “non-responsive” drips tend to focus around the periphery. This suggests some relationship between drip hydrology and the cave chamber morphology and lithology through which drip flow paths are routed.

Clusters with larger distances (for example > 40) should be treated with caution, especially if the mean correlation is low and offset is high. The so called “non-responsive” drips (280, 369, 352, 321, 372 in Fig. 4) tend to form parts of these less compact

Table 2. MDS clusters along with their cluster parameters of mean distance within each cluster; mean correlation coefficient within the cluster and mean offset within the cluster.

		MDS Cluster Group			
		1	2	3	4
All data		369	321, 325, 329, 332, 342, 348, 372, 395, 396	279, 280, 357, 370, 374, 376, 379	326, 352
Cluster properties:	Mean distance (no units):	N/A	25.5	7.3	185.2
	Mean *r* value:	N/A	0.63	0.49	0.02
	Mean offset (hrs):	N/A	63.0	9.5	202.0
Filtered		352, 379	280, 348, 369, 374	279, 321, 325, 329, 332, 342, 357, 370, 376, 395, 396	326, 372
Cluster properties:	Mean distance (no units):	12.6	45.9	28.8	44.4
	Mean *r* value:	0.20	0.25	0.60	0.40
	Mean offset (hrs):	16.0	56.2	78.8	75.0

clusters (with the exception of 321), confirming the disconnect nature of many of these drips to the flow routes of cluster 3 in either set of MDS analyses (i.e. with or without the extreme values), and from each other. These drip sites often drip just once or twice a day and most likely are fed from distinct stores of water that now have little connection to other stores of groundwater or direct connections to surface infiltration, as indicated by the lack of consistent and believable clustering and low correlations to surface recharge in Fig. 5a and c.

One consistent feature that appears from the cluster analysis of Fig. 6 is the spatial heterogeneity of the clusters. Drips can have similar behaviour (well correlated together with a small lag), and still be far apart spatially. In particular cluster 3 is spatially scattered, indicating multiple fractures and an overall strong heterogeneity of the flow paths between the surface and the drips. The exact routing of water via numerous stores and interconnected fracture networks, results in a complex and often non-linear response of any individual drip to initial surface inputs.

CONCLUSIONS

These data demonstrate variability between drip rate time series at high spatial density of sampling. We observe evidence of two-phase flow as previously reported in French and British caves, but this is not a dominant direct influence on drip rates at the majority of sites. At this site and typically throughout SE Australia, there is a limited soil store along with high rates of evapotranspiration. The doline surface formation above south passage enables the generally limited recharge to be focussed to this section of the cave. MDS and clustering appears to indicate one major cluster of similarity in drip rate data that makes sense in the context of the observed cave chamber morphology, lithology. Specifically the presence of fossil flowstone comprising much of the cave chamber roof in South Passage and the unknown numbers of palaeokarst stores are key in understanding drip response to P-E and the spatial variability of drip behaviour throughout Cathedral cave. This fossil flowstone must predate previously reported groundwater dissolution events thought to be crucial in cave formation in this region and have enough matrix storage capacity capable of holding water throughout periods of reduced soil moisture and maintaining drips inside South Passage throughout the year. Specifically from the MDS we observe:

A range of drip responses that cannot be described by the existing models of vadose, shaft or seepage flows. Many of these responses have been observed in single drip studies as described earlier, but this is the first time that such a large spatial density of drips have been monitored enabling the application of an approach such as MDS.

A cluster of drips that are well correlated to the extreme recharge events and demonstrate a dual flow regime, where some fractures are only activated with high levels of saturation and extreme recharge. Spatially these drips occur beneath the shallow doline depression at the surface above the cave which likely acts to focus surface recharge to this portion of the cave, and hence explain the relative richness in active speleothem formation in this portion of the cave.

Despite a relatively shallow depth (30m), many drips appear to be fed from groundwater stores which are isolated from infiltration and other stores of water described above. Multiple cave development with

pockets of palaeokarst and sediment fill are likely sources, and as such these drips represent slow depletion at a steady rate over this monitoring period, and a primary porosity or matrix storage that is distinct to waters feeding other drips in South Passage.

MDS may therefore be concluded to be a suitable means by which to classify drip behaviour and will be the focus of future publications using a larger dataset of drip loggers, the collection of which was ongoing at the time of publication. The monitoring of drip rates has since been expanded to include many more drip loggers as well as tracers of stable isotopes (O and H) and temperature. These data will be the focus of future publications to expand the possibility of classifying drip regimes.

ACKNOWLEDGEMENTS

The authors acknowledge DIISR for Groundwater EIF, funding from the National Centre for Groundwater Research and Training (NCGRT), Greg Ryan for surveying, the SUSS for permission to use excerpts of the caves survey, Wellington Council and staff at Wellington Caves. We thank Mike Augee for providing information on soil and vegetation cover at the cave site. Finally we thank Pierre-Yves Jeannin and two anonymous reviewers for their constructive and considered comments that have greatly improved the manuscript.

REFERENCES

Acworth R. & Brain T., 2008 - *Calculation of barometric efficiency in shallow piezometers using water levels, atmospheric and earth tide data*. Hydrogeology Journal, **16**: 1469-1481. http://dx.doi.org/10.1007/s10040-008-0333-y

Arbel Y., Greenbaum N., Lange J., & Inbar M., 2010 - *Infiltration processes and flow rates in developed karst vadose zone using tracers in cave drips*. Earth Surface Processes and Landforms, **35**: 1682-1693. http://dx.doi.org/10.1002/esp.2010

Baker A. & Brunsdon C., 2003 - *Non-linearities in drip water hydrology: an example from Stump Cross Caverns, Yorkshire*. Journal of Hydrology, **277**: 151-163. http://dx.doi.org/10.1016/S0022-1694(03)00063-5

Baker A. & Fairchild I.J., 2012. - *Drip Water Hydrology and Speleothems*. Nature Education Knowledge,3(5):16.

Borg I. & Groenen P., 1997 - *Modern multidimensional scaling: theory and applications*. Springer New York, 614 p.

Collister C. & Mattey D., 2008 - *Controls on water drop volume at speleothem drip sites: An experimental study*. Journal of Hydrology, **358**: 259-267. http://dx.doi.org/10.1016/j.jhydrol.2008.06.008

Cox T.F. & Cox M.A.A., 1994 - *Multidimensional Scaling*. Boca Raton, FL: CRC/Chapman and Hall.

Fernández-Cortés A., Calaforra J.M., Sánchez-Martos F. & Gisbert J., 2007 - *Stalactite drip rate variations controlled by air pressure changes: an example of non-linear infiltration processes in the 'Cueva del Agua' (Spain)*. Hydrological Processes, **21**: 920-930.

Frank R., 1971 - *The clastic sediments of the Wellington Caves, New South Wales*. Helictite, **9**: 3-34.

Frank R., 1975 - *Late Quaternary climatic change: evidence from cave sediments in central eastern New South Wales*. Australian Geographical Studies, **13**: 154-168. http://dx.doi.org/10.1111/j.1467-8470.1975.tb00164.x

Fuller L., Baker A., Fairchild I.J., Spötl C., Marca-Bell A., Rowe P. & Dennis P.F., 2008 - *Isotope hydrology of dripwaters in a Scottish cave and implications for stalagmite palaeoclimate research*. Hydrology and Earth System Sciences, **12**: 1065-1074. http://dx.doi.org/10.5194/hess-12-1065-2008

Genty D. & Deflandre G., 1998 - *Drip flow variations under a stalactite of the Père Noël cave (Belgium). Evidence of seasonal variations and air pressure constraints*. Journal of Hydrology, **211**: 208-232. http://dx.doi.org/10.1016/S0022-1694(98)00235-2

Gunn J., 1974 - *A model of the karst percolation system of waterfall swallet, Derbyshire*. Transactions of the British Cave Research Association, **3**: 159-164.

Kaufman A., Bar-Matthews M., Ayalon A. & Carmi I., 2003 - *The vadose flow above Soreq Cave, Israel: a tritium study of the cave waters*. Journal of Hydrology, **273**: 155-163. http://dx.doi.org/10.1016/S0022-1694(02)00394-3

Kluge T., Riechelmann D.F.C., Wieser M., Spötl C., Sültenfuß J., Schröder-Ritzrau A., Niggemann S. & Aeschbach-Hertig W., 2010 - *Dating cave drip water by tritium*. Journal of Hydrology, **394**: 396-406. http://dx.doi.org/10.1016/j.jhydrol.2010.09.015

Maurice L., Atkinson T.C., Williams A.T., Barker J.A. & Farrant A.R., 2010 - *Catchment scale tracer testing from karstic features in a porous limestone*. Journal of Hydrology, **389**: 31-41. http://dx.doi.org/10.1016/j.jhydrol.2010.05.019

Miorandi R., Borsato A., Frisia S., Fairchild I.J. & Richter D.K., 2010 - *Epikarst hydrology and implications for stalagmite capture of climate changes at Grotta di Ernesto (NE Italy): results from long-term monitoring*. Hydrological Processes, **24**: 3101-3114. http://dx.doi.org/10.1002/hyp.7744

Osborne R.A.L., 2007 - *Cathedral Cave, Wellington Caves, New South Wales, Australia. A multiphase, non-fluvial cave*. Earth Surface Processes and Landforms, **32**: 2075-2103. http://dx.doi.org/10.1002/esp.1507

Perrin J., Jeannin P.-Y. & Zwahlen F., 2003 - *Implications of the spatial variability of infiltration-water chemistry for the investigation of a karst aquifer: a field study at Milandre test site, Swiss Jura*. Hydrogeology Journal, **11**: 673-686.

Pitty A.F., 1966 - *An approach to the study of karst water*. University of Hull Occasional Papers in Geography, **5**.

Pitty A.F., 1968 - *Calcium carbonate content of karst water in relation to flow-through time*. Nature, **217**: 939-940. http://dx.doi.org/10.1038/217939a0

Scheidt C. & Caers J., 2009 - *Representing Spatial Uncertainty Using Distances and Kernels*. Mathematical Geosciences, **4**: 397-419. http://dx.doi.org/10.1007/s11004-008-9186-0

Shapiro A., 2011 - *The challenge of interpreting environmental tracer concentrations in fractured rock and carbonate aquifers*. Hydrogeology Journal, **19**: 9-12. http://dx.doi.org/10.1007/s10040-010-0678-x

Sheffer N.A., Cohen M., Morin E., Grodek T., Gimburg A., Magal E., Gvirtzman H., Nied M., Isele D. & Frumkin A., 2011 - *Integrated cave drip monitoring for epikarst recharge estimation in a dry Mediterranean area, Sif Cave, Israel*. Hydrological Processes, **25**: 2837-2845. http://dx.doi.org/10.1002/hyp.8046

Smart P.L. & Friederich H., 1987 *Water movement and storage in the unsaturated zone of a maturely karstified carbonate aquifer, Mendip Hills, England* Proceedings of the Environmental Problems in Karst Terranes and their Solutions Conference, KY, USA, pp. 57-87.

Spath H., 1985 - *Cluster dissection and analysis: Theory, FORTRAN programs examples*. Halsted Press, New York, 226 p.

Thornthwaite C.W. & Mather J.R., 1957 - *Instructions and Tables for Computing Potential Evapotranspiration and the Water Balance*. Drexel Institute of Technology, Laboratory of Climatology, Publications in Climatology, **10**: 185-311.

Verheyden S., Genty D., Deflandre G., Quinif Y. & Keppens E., 2008 - *Monitoring climatological, hydrological and geochemical parameters in the Père Noel cave (Belgium): implication for the interpretation of speleothem isotopic and geochemical time-series*. International Journal of Speleology, **37**: 221-234.

Worthington S.R.H. & Ford D.C., 2009 - *Self-Organized Permeability in Carbonate Aquifers*. Ground Water, **47**: 326-336. http://dx.doi.org/10.1111/j.1745-6584.2009.00551.x

Worthington S.R.H. & Gunn J., 2009 - *Hydrogeology of Carbonate Aquifers: A Short History*. Ground Water, **47**: 462-467. http://dx.doi.org/10.1111/j.1745-6584.2008.00548.x

Supplementary Information:

Table S1. Descriptive statistics of drip logger data.

Logger Number:	279	280	321	322	325	326	329	332	333	342	348	352	357	369	370	372	374	376	379	395	396
Skew	9	1	0	39	2	1	0	0	16	0	0	0	3	5	9	0	1	18	3	0	2
Standard deviation	111	0	0	10	2	7	2	188	0	2	1	0	2	0	7	0	17	23	2	1	1
Mean	37	1	1	1	3	6	2	261	0	3	2	1	1	0	2	1	19	8	3	7	2
Min	0	0	0	0	0	0	0	0	0	0	0	0	0	0	0	0	0	0	1	4	0
25th percentile	2	1	1	0	1	0	1	84	0	1	1	1	0	0	0	1	4	2	2	6	1
Median	7	1	1	0	3	1	2	277	0	2	2	1	1	0	1	1	14	6	3	7	1
75th percentile	34	1	1	0	4	14	3	448	0	5	3	2	2	0	1	1	34	9	4	8	2
Max	1455	2	2	526	19	57	10	580	7	8	4	3	19	1	71	2	89	548	16	11	6

Figure S1. Daily total drip rate time series.